Advances in Energy Science and Technology
Vol. 1, No. 2|1 September 2025
AEST

A Theoretical examination of source back-scattering, self-absorption phenomena, and size evaluation in betavoltaic cells

Hassan Fathi [a], **Hossein Afarideh** [a,*], **Fereydoun Abbasi Davani**[b], **Mina Amirmazlaghani**[c]

[a] *Department of Energy Engineering and Physics, Amirkabir University of Technology, No. 350, Hafez Ave, Valiasr Square, Tehran 15875-4413, Iran*

[b] *Radiation Application Department, Shahid Beheshti University, Shahid Shahriari Square, Evin, Tehran 1983969411, Iran*

[c] *Nano Electronics Lab (NEL), Shahid Rajaee Teacher Training University, Shahid Shabanlou St., Lavizan, Tehran 16785-163, Iran*

Keywords

Betavoltaic cell
Self-absorption
Backscattering effect
Size limitations
$^{147}Pm_2O_3/Si$

Article Info

DOI: 10.22060/aest.2025.5790

Received date 18 April 2025

Accepted date 22 June 2025

Published date 1 September 2025

* **Corresponding author:**
hafarideh@aut.ac.ir

Abstract

The effect of source backscattering and self-absorption on the basic parameters of a $^{147}Pm_2O_3/Si$ planar betavoltaic devices is covered. Calculations show that self-absorption loss can reach up to 31.579% of the actual activity and overall efficiency can be reduced from 4.361% to 4.274%. If self-absorption and source backscattering are considered together it is observed that the source backscattering factor compensates to some extent the reduction of the actual activity induced by the self-absorption and ultimately, overall conversion efficiency can reach up to 4.352%. Also, as a case study lower bounds on the size of planar and spherical betavoltaic cells are reported. Further, the effect of parameters such as nominal source curie content, the total number of fuel atoms in the division's volume, total power released by the source, the maximum energy of beta particles, and semiconductor density in the size of the nuclear battery was investigated.

Graphical Abstract

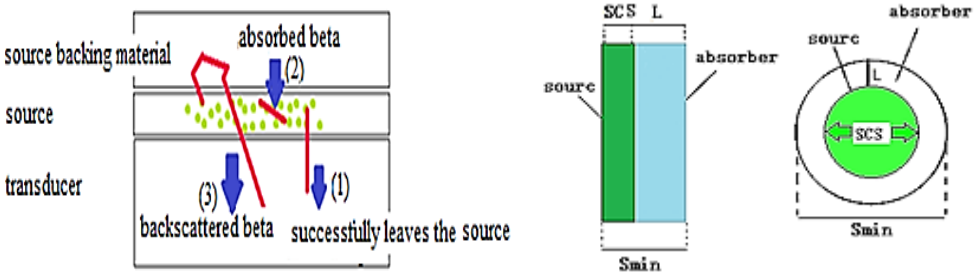

Advances in Energy Science and Technology
Vol. 1, No. 2|1 September 2025
AEST

1. Introduction

The utilization of energy from radioisotope decay serves a crucial role in the production of consistent and reliable electricity. A betavoltaic device generates electrical current by converting the kinetic energy from beta radiation into electricity [1]. Beta particles passing through a semiconductor create an ionization trail, which generates electron-hole pairs within the semiconductor's bulk material. An early attempt at betavoltaic conversion can be traced back to 1953[2]. From the mid-1960s through the 1990s, researchers explored and evaluated various betavoltaic technologies for a range of potential uses [3-7]. Since the 1990s, scientists have explored various concepts and extended the longevity of cells. [8-14]. In nuclear cells, the radioisotope serves as a crucial performance element, functioning as the battery's energy source. Energy losses occur within the source material due to self-absorption as particles move, diminishing efficiency from its optimal level. To maximize energy deposition in the transducer, the ionizing particle must exit the source with minimal self-absorption. The backing material supporting the source also plays a significant role in determining source efficiency, alongside self-absorption.

This paper is structured as follows: after a concise overview of self-absorption, an examination of how source material thickness impacts energy loss from self-absorption is conducted for beta particles from five different sources, both qualitatively and quantitatively. The third section explores source backscattering and its influencing factors, including beta particle energy and backing material atomic number. Section four addresses the effects of source backscattering and self-absorption on key parameters of standard planar betavoltaic devices. Additionally, this study presents theoretical calculations on the size limitations of planar and spherical 147-Pm betavoltaic cells and their relationship to the source's maximum energy storage and output power. The final two sections provide concluding remarks.

2. Materials and Methods

2.1. Source self-absorption (f_{self})

Beta particles originating from lower layers are partially absorbed by the source material, regardless of its thickness. This phenomenon, known as self-absorption or self-scattering, is influenced by factors such as chemical composition, density, device geometry, effective atomic number, layer thickness, and maximum beta particle energy. The self-absorption factor of a beta source (f_{self}) is defined as the proportion of beta particles undergoing self-absorption, represented by a dimensionless value between 0 and 1 [15-17]. It can be expressed in the following form:

$$f_{self} = \left[1 - \left(\frac{1-e^{-\mu t}}{\mu t}\right)\right].100\% \quad (1)$$

$$\mu = 1.7/(E_{\beta,max}^{1.14})$$

where μ is the mass absorption coefficient (m^2/kg), t is the thickness of the beta source (kg/m^2).

As shown in **Fig. 1**, particles 1 and 3 may be converted to an electric current, while particle 2 does not have this capability due to self-absorption. Therefore, this phenomenon negatively affects the current and, consequently, other key parameters of the battery. **Fig. 2** illustrates how self-absorption loss varies with beta source thickness. **Table 1** outlines the parameters for ^{3}H, ^{63}Ni, ^{35}S, ^{147}Pm, and ^{90}Sr. Two conclusions can be drawn from **Fig. 1**: firstly, the self-absorption loss for each source material initially rises rapidly as source thickness increases before reaching a plateau; secondly, radioactive materials with low beta energies, such as ^{63}Ni and ^{3}H, are more susceptible to the self-absorption phenomenon.

Advances in Energy Science and Technology
Vol. 1, No. 2|1 September 2025
AEST

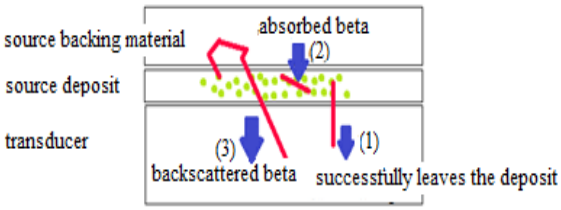

Fig. 1. Particle 1 is directed towards the transducer, while particle 2 is retained within the source, preventing its conversion into electrical energy. Particle 3 is released in the reverse direction. In the absence of the source's backing, this particle would not return. However, when the backing material is in place, there exists a potential for the second particle to undergo scattering interactions, which may alter its trajectory and allow it to enter the p-n junction.

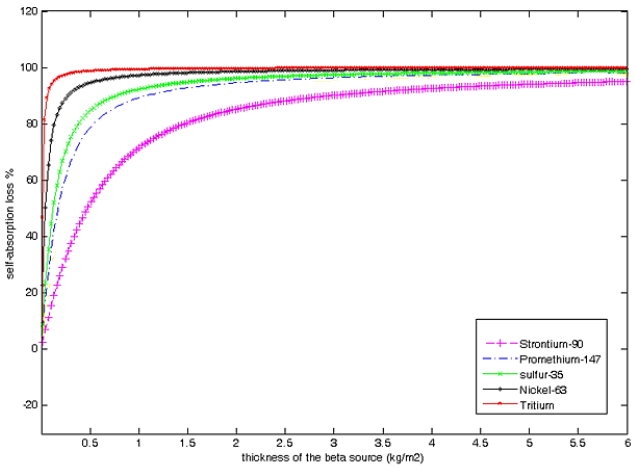

Fig. 2. The dependence of self-absorption loss on the thickness of the beta source.

Table 1. Characteristics of several betavoltaic sources.

Parameter	Tritium	Nickel-63	Sulfur-35	Promethium-147	Cobalt-60	Strontium-90
Maximum energy of the beta particle (*keV*)	18.61	67	167	225	318	546
Average energy of the beta particle (*keV*)	5.7	17.4	49	73	97	195.8
Density (kg/m^3)	2330	8900	1600	6475	8900	2640

2.2. Ionization and excitation stopping power

Beta particles lose their energy through the coulomb interaction with electrons/nuclei and emission of electromagnetic radiation (Bremsstrahlung). The mean energy dissipated per unit distance traversed by the particle can be expressed as follows [18]:

$$\left(\frac{dE}{dx}\right)_{ion}\left(\frac{MeV}{m}\right) = 4\pi r_0^2 \frac{mc^2}{\beta^2} NZ\left\{Ln\left(\frac{\beta\gamma\sqrt{\gamma-1}}{I}mc^2\right) + \frac{1}{2\gamma^2}\left[\frac{(\gamma-1)^2}{8} + 1 - (\gamma^2 + 2\gamma - 1)Ln2\right]\right\}, \quad (2)$$

where $(\frac{dE}{dx})_{ion}$ represents the ionization and excitation stopping power for beta particles in *Mev/m*, c is the speed of light (3×10^8 *m/sec*), r_0 is the electron radius (2.818×10^{15} *m*), Z is the material's atomic number, N is the atomic density (*atom/*

m^3), β is the particle's relative phase velocity, m is the electron mass (9.109×10^{31} kg), γ is the Lorentz factor and I is the absorbing medium's mean excitation potential in eV. An approximate equation for I, yielding accurate results for Z>12, is:

$$I(eV) = (9.76 + 58.8Z^{-1.19})Z. \quad (3)$$

2.3. Bremsstrahlung emission stopping power

The relation between the loss of energy due to Bremsstrahlung emission and the loss associated with Coulomb interactions can be articulated through the following equation.

$$(\frac{dE}{dx})_{rad} = \frac{ZT(MeV)}{750}\left(\frac{dE}{dx}\right)_{ion}. \quad (4)$$

In this equation, Z denotes the atomic number, while E signifies the energy measured in MeV. The overall stopping power for beta particles is derived from the combination of the two equations, specifically **Eqs. (2)** and **(4)**, leading to the expression:

$$(\frac{dE}{dx})_{tot} = (\frac{dE}{dx})_{ion} + (\frac{dE}{dx})_{rad} = \left(1 + \frac{ZT}{750}\right)\left(\frac{dE}{dx}\right)_{ion}. \quad (5)$$

2.4. Energy loss after traversing a material of thickness t<R

When assessing the energy loss of a beta particle as it moves through a material of thickness t, it is essential to first determine the particle's range within that specific medium. If the range R is less than the thickness t, the beta particle will be completely absorbed by the material, resulting in a total energy loss that corresponds to the particle's initial energy. Conversely, if the range R exceeds the thickness t, the energy loss ΔE is given by:

$$\Delta E = \int_0^t (\frac{dE}{dx})_{tot} dx. \quad (6)$$

If $t \ll R$,, it is permissible to consider $(\frac{dE}{dx})_{tot}$ as a constant value and obtain:

$$\Delta E = \left(\frac{dE}{dx}\right)_{tot-0} t. \quad (7)$$

The term $(\frac{dE}{dx})_{tot-0}$ refers to the stopping power determined at the particle's initial energy. When the thickness t represents a significant portion of the particle's range, it is inappropriate to assume that $(\frac{dE}{dx})_{tot}$ remains constant; thus, a numerical integration approach becomes necessary to accurately assess the energy loss. In **Table 2**, the total energy losses are presented for five different source materials, all maintained at an identical thickness of d=12.09 μm. For the purposes of this analysis, the radioactive sample is treated as being infinitely thin, which implies that its thickness is negligible compared to the range (i.e., t≪R). According to **Table 2**, it can be seen that the minimum and maximum energy losses for t=12.09 μm are 0.00561522833 and 0.225567189 MeV for strontium-90 and tritium, respectively.

Table 2. The attenuation of beta particle's energy as it passes through a material of thickness t.

Parameter	Tritium	Nickel-63	Sulfur-35	Promethium-147	Strontium-90
$(\frac{dE}{dx})_{ion}\left(\frac{MeV}{m}\right)$	18657.1939	8387.39726	838.542	1729.951	459.889948
$(\frac{dE}{dx})_{rad}\left(\frac{MeV}{m}\right)$	0.141794674	5.44845326	0.876555901	10.2712957	4.56235356
$(\frac{dE}{dx})_{tot}\left(\frac{MeV}{m}\right)$	18657.3357	8392.84571	839.418556	1740.2223	464.452302
$\Delta E(MeV)$ (t=12.09μm)	0.225567189	0.101469505	0.0101485703	0.0210392876	0.00561522833

2.5. Source backscattering factor (f_b)

The phenomenon of backscattering from a source support exhibits an increase in intensity as the thickness of the backing material rises, ultimately reaching a saturation point. This saturation occurs when the thickness of the backing approaches approximately one-fifth of the extrapolated range of beta particles within that specific material, denoted as $b_s=b(saturation) \approx 0.2R$. The relationship between the saturation backscattering factor of beta particles and the energy, as well as the atomic number of the backing material, can be effectively characterized through an empirical equation [17,19]:

$$f_b(sat) = 1 + \frac{b_1 \exp(-b_2 Z^{-b_3})}{1+(b_4+b_5 Z^{-b_6})\alpha^{\left(b_7-\frac{b_8}{Z}\right)}}, \quad (8)$$

$b_1 = 1.15 \pm 0.06;\ b_2 = 8.35 \pm 0.25;\ b_3 = 0.525 \pm 0.02;$

$b_4 = 0.0185 \pm 0.0019;\ b_5 = 15.7 \pm 3.1;\ b_6 = 1.59 \pm 0.07;\ b_7 = 1.56 \pm 0.02;$

$b_8 = 4.42 \pm 0.18\ ;\ \alpha = E_{\beta,max}/mc^2.$

The relationship between $f_b(sat)$ and beta energy for five elements is illustrated in **Fig. 3**. It is evident that as the energy of beta particles rises, there is a corresponding decline in backscattering. This trend indicates that higher energy beta particles are more likely to escape from the backing material.

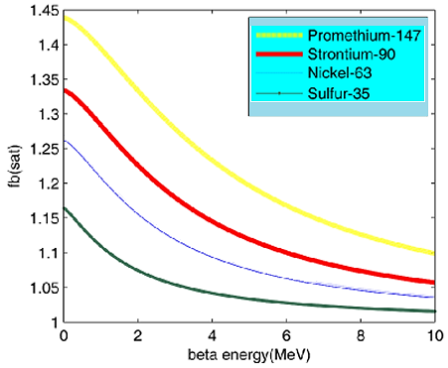

Fig. 3. The dependence of the backscattering factor on energy for 147-Pm, 90-Sr, 63-Ni, and 35-S. Curves were obtained using **Eq. (8)**.

In **Fig. 4**, the relationship between the saturation backscattering factor and the atomic number of the backing material is illustrated for five distinct beta energies. The analysis assumes that the radioactive sample is infinitely thin, thereby eliminating any effects of self-absorption. Notably, the data for Nickel-63 ($Z= 28$) indicates that approximately 20% of the radiation detected in the p-n junction can be attributed to back-scattered radiation (0.25/ (1.0 + 0.25) = 0.2).

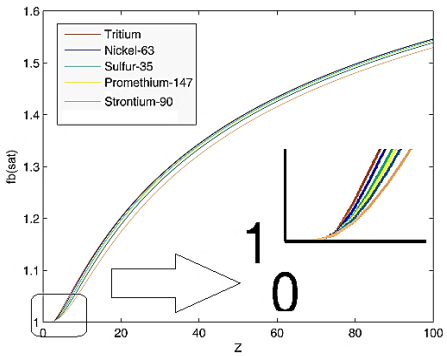

Fig. 4. The relationship between the saturation backscattering factor and the atomic number *Z* of the backing material.

2.6. Effect of source backscattering and self-absorption on the basic parameters of conventional planar betavoltaic devices

This section aims to elucidate the influence of the source self-absorption and backing material on the fundamental parameters of a cell. The significance of both effects is consistently paramount in the assessment of device efficiency. The betavoltaic cell under discussion is constructed using a promethium oxide source in conjunction with a silicon p-n diode.

Pm147 presents itself as a suitable option for application in nuclear batteries, primarily attributed to its advantageous power density of 15 $\mu W/cm^2$ derived from Pm_2O_3. It emits a minimal quantity of low-energy gamma photons, which significantly reduces potential health hazards. The chemical form of promethium is exhibited in oxide form, Pm_2O_3. The parameter values for the source and semiconductor have been sourced from the works of [20-21] and are tabulated in **Table 1**. In the following, we set the basic battery parameters in three modes (without self-absorption, with self-absorption, and with both self-absorption and backscattering), the effect of both phenomena on these parameters is shown, and finally, conversion efficiency is calculated in each case.

2.6.1. Beta current at the surface of the planar source

The current resulting from beta emission at each surface of the planar source can be expressed as follows [5]:

$$I_\beta^s = \frac{3.7\times10^{10}qH\rho A}{2\alpha_0}(1-e^{-\alpha_0 t}), \tag{9}$$

where α_0 (cm^{-1}), and ρ (g/cm^3) are the self-absorption coefficient and density of the Pm_2O_3, q is the charge of an electron (c), H is the specific activity (Ci/g), is the density of the source A is the area of the cell (cm^2 and t is the thickness of the slab (cm). Regardless of the self-absorption effect, I_β can be written as follows:

$$I_\beta = \frac{3.7\times10^{10}qH\rho V}{2}, \tag{10}$$

where V is the volume of the source (cm^3). With both self-absorption and source backscattering, the beta emission current can be described as follows:

$$I_\beta^{s-b} = \frac{3.7\times10^{10}qH\rho A}{2\alpha_0}f_b(1-e^{-\alpha_0 t}). \tag{11}$$

2.6.2. Beta current at the p-n junction

When the promethium source is positioned in proximity to the semiconductor surface, a significant portion of the emitted beta particles penetrates the semiconductor material, while a fraction is reflected back towards the source. Therefore, the beta current at the p-n junction is [5]:

$$i_\beta^s\left(i_\beta \text{ or } i_\beta^{s-b}\right) = I_\beta^s\left(I_\beta \text{ or} I_\beta^{s-b}\right)e^{-\alpha x}(1-\gamma). \tag{12}$$

In this context, α represents the absorption coefficient of the semiconductor, measured in units of (cm^{-1}), while γ denotes the reflection coefficient. To calculate the reflection coefficient, one can apply the following formula [22]:

$$\gamma = \frac{Ln(Z_{eff})}{6} - 0.25, \tag{13}$$

where Z_{eff} is the effective atomic number of the reflected surface material. Beta particles penetrating into the absorbent material lose energy, so their chance of transmission decreases. This is illustrated in **Fig. 5**.

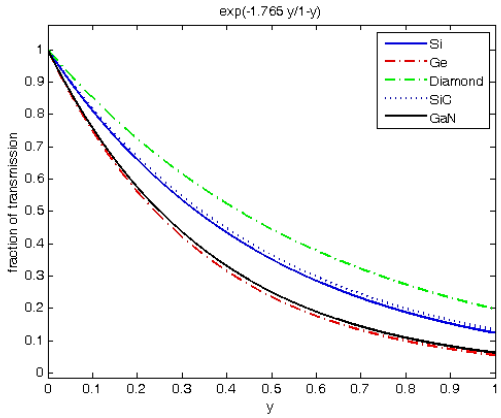

Fig. 5. The relationship between the transmission fraction and the depth y of the absorbing material across various semiconductor types.

2.6.3. The generation rate of electron-hole pairs in the semiconductor

The generation rate of electron-hole pairs in the semiconductor material is given by [5]:

$$G^s(x)\left(\, G(x)\ or G^{s-b}(x)\right) = \frac{m}{q}\left|\frac{di_\beta^s\left(di_\beta\ or\ di_\beta^{s-b}\right)}{dx}\right|, \tag{14}$$

where m is the multiplication factor, can be expressed by:

$$m = \frac{E_{av}}{w}. \tag{15}$$

2.6.4. Short circuit current density

The short circuit current density (A/cm^2) for three cases (by considering self-absorption phenomena, without considering self-absorption effect, and by taking into account both self-absorption and back-scattering factors) is given by the following relationships, respectively [23]:

$$J_{SC}^s = \int_0^L C_{eff}(1-\gamma)\frac{\left[3.7\times10^{10}H\rho\left(1-e^{-\alpha_0 t}\right)m\alpha\right]}{2\alpha_0}e^{-\alpha x}dx, \tag{16}$$

$$J_{SC} = \int_0^L C_{eff}(1-\gamma)\frac{\left[3.7\times10^{10}H\rho m\alpha d\right]}{2}e^{-\alpha x}dx, \tag{17}$$

and

$$J_{SC}^{s-b} = \int_0^L C_{eff}f_b(1-\gamma)\frac{\left[3.7\times10^{10}H\rho\left(1-e^{-\alpha_0 t}\right)m\alpha\right]}{2\alpha_0}e^{-\alpha x}dx, \tag{18}$$

Where C_{eff} is the electron-hole pair collection efficiency.

2.6.5. Open-circuit voltage

The Shockley equation provides a mathematical representation of the open-circuit voltage (V_{oc} in V) for an ideal p-n junction. This equation is written as follows [2]:

$$V_{OC}^s(V_{OC}\ or\ V_{OC}^{s-b}) = \frac{kT}{q}Ln\left(\frac{J_{SC}^s\left(J_{sc}\ or J_{SC}^{s-b}\right)}{1.5\times10^5\exp(-E_g/kT)}\right), \tag{19}$$

where k indicates the Boltzmann constant 8.617×10^{-5} eVK^{-1}, T is the temperature in Kelvin.

2.6.6. Fill Factor

The other factor in determining the basic betavoltaic cell is the Fill Factor, which is written as [24]:

$$FF^{s}(\,FFor FF^{s-b}\,)=\frac{\left[\left(\frac{V_{OC}^{s}\left(V_{OC}\,or\,V_{OC}^{s-b}\right)}{kT}\right)-Ln\left(\frac{V_{OC}^{s}\left(V_{OC}\,or\,V_{OC}^{s-b}\right)}{kT}+0.72\right)\right]}{\left[\left(\frac{V_{OC}^{s}\left(V_{OC}\,or\,V_{OC}^{s-b}\right)}{kT}\right)+1\right]}. \quad (20)$$

2.6.7. Observable activity of thin sample

The phenomenon of self-absorption results in a discrepancy between the observed activity and the true activity of the source, leading to a reduction in the apparent activity. Conversely, the observable activity can be augmented through reflection processes, which are attributed to backscattering effects. Thus, the apparent activity in both cases is described as:

$$Ci^{s}=\frac{Ci}{\alpha_0 t}(1-e^{-\alpha_0 t}), \quad (21)$$

$$Ci^{s-b}=\frac{Ci^{s}}{\alpha_0 t}f_b(1-e^{-\alpha_0 t}). \quad (22)$$

2.6.8. Source power

One can obtain the surface power density of the source as:

$$P_s^{s}(P_s or\ P_s^{s-b}\,)=3.7\times10^{10}qCi^{s}(C_i\ or\ Ci^{s-b})E_{av}. \quad (23)$$

2.6.9. Efficiency

The overall efficiency conversion is calculated as follows:

$$\eta^{s}(\eta\ or\ \eta^{s-b})=\frac{FF^{s}\times J_{SC}^{s}\times V_{OC}^{s}}{P_s^{s}}\left(\frac{FF\times J_{SC}\times V_{oc}}{P_s}\ or\ \frac{FF^{s-b}\times J_{SC}^{s-b}\times V_{OC}^{s-b}}{P_s^{s-b}}\right). \quad (24)$$

The parameters described in the previous sections are calculated for the planar betavoltaic cell in **Table 4**.

2.7. The lower bounds on the size of the planar and spherical 147-Pm betavoltaic cells

Although the size of the micro battery is important in understanding the issues and constraints for designing a battery, the topic of device scale frequently remains overlooked in nuclear battery concepts. This section presents an analysis of the size restrictions associated with planar and spherical 147-Pm betavoltaic cells, exploring how these limitations affect the maximum energy storage and output power capabilities that can be theoretically achieved.

The range of an electron, defined as the total distance L it travels through a material before depleting its energy, serves as a critical parameter in the context of betavoltaic transducers. This range represents a fundamental minimum size requirement for the transducer, influencing its design and efficiency. An approximation of the stopping range can be expressed as:

$$L\sim aE_{max}{}^{b}, \quad (25)$$

where a and b represent constants that are influenced by the characteristics and energy of the projectile particle, as well as the properties of the irradiated material. E_{max} denotes the highest energy that can be emitted by a radioactive atom.

The range at which beta particles from 147-Pm cease to travel in semiconductor materials L can be computed using the formula established by *Katz* and *Penfold* [25]:

$$L(cm)=\frac{0.412}{\rho\left(\frac{g}{cm^3}\right)}(E_{\beta,\max}(MeV)\,)^{1.265-0.0954Ln\left(E_{\beta,max}\right)}\quad 0.01\le E_{\beta,max}\le 2.5Mev, \quad (26)$$

where ρ is the density of the semiconductor and $E_{B,max}$ is the maximum energy of beta particles.

In 1972, *Tabata*, *Ito*, and *Okabe* [17] introduced another semiempirical equation that delineates the range of electrons for energy levels between 0.3 *keV* to 30 *MeV*, based on the experimental data that had been compiled until that time. This equation is formulated as follows:

$$L(m) = \frac{a_1}{\rho\left(\frac{kg}{m^3}\right)}\left(\frac{Ln[1+a_2(\gamma-1)]}{a_2} - \frac{a_3(\gamma-1)}{1+a_4(\gamma-1)^{a_5}}\right), \quad (27)$$

$$a_1 = \frac{2.335A_W(g)}{Z^{1.209}}, a_2 = 1.78\times10^{-4}Z, a_3 = 0.9891 - (3.01\times10^{-4}Z),$$

$$a_4 = 1.468 - (1.180\times10^{-2}Z), a_5 = \frac{1.232}{Z^{0.109}}, \gamma = \frac{T(\text{MeV}) + 0.511}{0.511},$$

where Z represents the atomic number of the substance in question, the kinetic energy of the electron is denoted by T, while A_W is the atomic weight. To estimate the range of the electron within the material, a third formula can be expressed as follows [26]:

$$L(cm) = \frac{0.407(E_{\beta,\max(MeV)})^{1.38}}{\rho(g/cm^3)}. \qquad E_{\beta,\max} \le 0.8MeV \quad (28)$$

The fourth relation that can be written for the beta range in the material given by *Kanayat–Okayama* (K–O):

$$L = \int_0^{E_0}\frac{dE}{dE/dx} = \frac{T^{5/3}}{\lambda_s\times5\times2^{5/3}\pi a^{1/3}e^{10/3}NZ}, \quad (29)$$

where *dE/dx* is the energy loss due to collisions, the number N is given by $Na\ \rho/Aw$, N_a is the Avogadro number, a is the effective screened radius of the atom, λ_s is a constant value, and e represents the electronic charge. As a result, the mass-range ρL can be described by:

$$\rho L = 5.025\times10^{-12}\,A_W T^{5/3}/\lambda_s Z^{8/9}. \quad (30)$$

A notable consistency with experimental data in the range of 10 to 1000 *keV* is obtained by selecting λ_s=0.182. The equation denoted as **Eq. (30)** can be revised to incorporate relativistic corrections associated with energy and the effective screened radius of the atom:

$$L(cm) = \frac{2.76\times10^{-11}A_W(g)T(ev)^{\left(\frac{5}{3}\right)}}{\rho(g/cm^3)Z^{\left(\frac{8}{9}\right)}}\frac{(1+0.978\times10^{-6}T(ev))^{\left(\frac{5}{3}\right)}}{(1+1.957\times10^{-6}T(ev))^{\left(\frac{4}{3}\right)}}. \quad (31)$$

The beta particle range of the promethium oxide source in the converter substance (silicon) has been calculated using **Eqs. (26-28)** and **Eq. (30)** in **Table 5**.

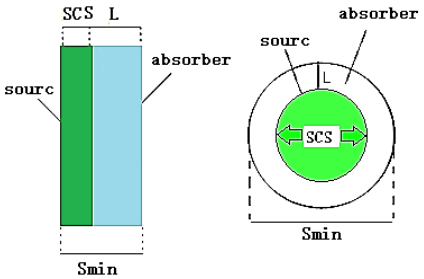

Fig. 6. The lower bounds on the size of the planar (left) and spherical(right) 147-Pm betavoltaic cells.

For the planar cell configuration, the minimum size is defined as the sum of the source compartment size (SCS) and the semiconductor thickness L, expressed as S_{min}= $SCS + L$ (**Fig.6** (left)). In contrast, for the spherical cell, this minimum size parameter is represented as ($SCS + 2L$) (**Fig.6** (right)). The relationship between the stored energy and the output power of the source with SCS can be expressed by the following equation:

$$SCS_{planar\ cell} = \frac{P\tau mN_{Pm_2O_3}}{E_{av}\rho N_A A N_{Pm}}, \quad (32)$$

$$SCS_{spherical\ cell} = 2\left(\frac{3P\tau mN_{Pm_2O_3}}{4\pi E_{av}\rho N_A N_{Pm}}\right)^{\frac{1}{3}}, \quad (33)$$

Where P(=$3.7\times10^{10}CiE_{av}$) is the power of N radioactive atoms (W), τ is the average lifespan of a radioactive atom(sec), E_{av} represents the mean energy of beta particles (J), ρ is the density (g/cm^3), N_A is Avogadro's Number, N_{Pm} and $N_{Pm_2O_3}$ represent the number of promethium and promethium oxide atoms, respectively. A represents the area of the cell (cm^2), and m denotes the molar mass expressed in grams per mole ($g/mole$). Considering the above formulas, the lower bounds on the size of a planar cell are described by:

$$S_{min-planar\ cell}(\mathrm{I}) = \left[\frac{P\tau mN_{Pm_2O_3}}{E_{av}\rho N_A A N_{Pm}} + \frac{0.412}{\rho}E_{\beta,max}{}^{1.265-0.0954Ln(E_{\beta,max})}\right], \tag{34}$$

$$S_{min-planar\ cell}(\mathrm{II}) = \left[\frac{P\tau mN_{Pm_2O_3}}{E_{av}\rho N_A A N_{Pm}} + \frac{a_1}{\rho}\left(\frac{Ln[1+a_2(\gamma-1)]}{a_2} - \frac{a_3(\gamma-1)}{1+a_4(\gamma-1)^{a_5}}\right)\right], \tag{35}$$

$$S_{min-planar\ cell}(\mathrm{III}) = \left[\frac{P\tau mN_{Pm_2O_3}}{E_{av}\rho N_A A N_{Pm}} + \frac{0.407(E_{\beta,\max})^{1.38}}{\rho}\right], \tag{36}$$

Or

$$S_{min-planar\ cell}(\mathrm{IV}) = \left[\frac{P\tau mN_{Pm_2O_3}}{E_{av}\rho N_A A N_{Pm}} + \frac{2.76\times10^{-11}A_W(g)T(ev)^{\left(\frac{5}{3}\right)}}{\rho Z^{\left(\frac{8}{9}\right)}}\frac{\left(1+0.978\times10^{-6}T(ev)\right)^{\left(\frac{5}{3}\right)}}{\left(1+1.957\times10^{-6}T(ev)\right)^{\left(\frac{4}{3}\right)}}\right]. \tag{37}$$

The lower bounds on the size of a spherical cell are:

$$S_{min-spherical\ cell}(\mathrm{I}) = 2\left[\left(\frac{3P\tau mN_{Pm_2O_3}}{4\pi E_{av}\rho N_A N_{Pm}}\right)^{\frac{1}{3}} + \frac{0.412}{\rho}E_{\beta,max}{}^{1.265-0.0954Ln(E_{\beta,max})}\right], \tag{38}$$

$$S_{min-spherical\ cell}(\mathrm{II}) = 2\left[\left(\frac{3P\tau mN_{Pm_2O_3}}{4\pi E_{av}\rho N_A N_{Pm}}\right)^{\frac{1}{3}} + \frac{a_1}{\rho}\left(\frac{Ln[1+a_2(\gamma-1)]}{a_2} - \frac{a_3(\gamma-1)}{1+a_4(\gamma-1)^{a_5}}\right)\right], \tag{39}$$

$$S_{min-spherical\ cell}(\mathrm{III}) = 2\left[\left(\frac{3P\tau mN_{Pm_2O_3}}{4\pi E_{av}\rho N_A N_{Pm}}\right)^{\frac{1}{3}} + \frac{0.407(E_{\beta,\max})^{1.38}}{\rho}\right], \tag{40}$$

Or

$$S_{min-spherical\ cell}(\mathrm{IV}) = 2\left[\left(\frac{3P\tau mN_{Pm_2O_3}}{4\pi E_{av}\rho N_A N_{Pm}}\right)^{\frac{1}{3}} + \frac{2.76\times10^{-11}A_W(g)T(ev)^{\left(\frac{5}{3}\right)}}{\rho Z^{\left(\frac{8}{9}\right)}}\frac{\left(1+0.978\times10^{-6}T(ev)\right)^{\left(\frac{5}{3}\right)}}{\left(1+1.957\times10^{-6}T(ev)\right)^{\left(\frac{4}{3}\right)}}\right]. \tag{41}$$

Using these formulas, **Eqs. (34-41)**, one can calculate the minimum possible size of each cell with the specific source and transducer parameters (**Table 6**). In the calculations, it is assumed that the values of the nominal source curie content and the cell area are 2.8 Ci/cm^2 and 2.85 cm^2, respectively. The analysis presented herein is limited to the assessment of the source and transducer sizes, without incorporating the effects of shielding or the gap between the radioactive source and the PN junction. Such exclusions are pertinent, as they play a crucial role in influencing the dimensions of the battery. High-energy electrons, specifically those exceeding 0.5MeV, typically exhibit a linear and extended trajectory while demonstrating reduced specific ionization in air. Conversely, low-energy beta particles have a limited travel distance in air before they interact with the device. For instance, when the radiation source (63-Ni) is positioned at a distance of approximately 2 mm from a conventional planar betavoltaic cell, the overall efficiency of the cell diminishes by a factor of eleven compared to a scenario where the source is in direct contact with the surface [12]. Therefore, positioning the radioactive source closer to the betavoltaic surface enhances the generation of electrical energy.

3. Results and Discussion

The efficiency of the cell is significantly impacted by the percentage of self-absorption, which rises with increasing source material thickness, as illustrated in **Fig. 2**. A self-absorption loss of approximately 100% from ^{3}H, 95% from 63Ni, 85% from ^{35}S, and 80% from ^{147}Pm occurs when compared to a source mass thickness of 0.5 (kg/m^2) of each material. In contrast,

the self-absorption losses of 90% from 90Sr are 50%, which is completely consistent with earlier research [27]. Tritium releases beta particles with the lowest energy, while strontium releases the maximum energy. Thus, the self-absorption loss is least noticeable for strontium and most substantial for tritium. **Eq. (4)** states that the atomic number and the incident beta's energy both affect the amount of Bremsstrahlung loss. The maximum energy of the radioactive source utilized in the case of a betavoltaic cell is only 0.01861-0.546 *MeV*, as indicated by **Table 1**, which summarizes the features of the frequently used sources of betavoltaics. The proportion of radioactive loss attributed to Bremsstrahlung through collision loss is observed to be between 0.008% and 0.97%. As indicated in **Table 1**, the energy lost by beta particles traveling through the ^{90}Sr and ^{3}H sources per micrometer is 0.46 *kV* and 19 *kV*, respectively. Notably, these two sources exhibit the lowest and highest levels of self-absorption loss among those analyzed. This indicates that the self-absorption loss in ^{3}H is approximately 41 times greater than that in ^{90}Sr. The findings depicted in **Figs. 3-4** reveal that the energy of the beta particle and the atomic number of the backing material affect the saturation backscattering factor in markedly different ways. As the energy of beta particles is increased, the probability of their escape from the backing material rises, resulting in a diminished saturation backscattering factor. On the other hand, materials with a high atomic number are more effective at returning particles to their source.

Table 3. Basic parameters of the radioactive source and transducer.

average energy of beta particles (E*av*)	**maximum energy of beta particles (*Emax*)**	**Absorption coefficient in silicon (α)**	**self-absorption coefficient (α_0)**
73*keV*	230 *keV*	380 cm^{-1}	1300 nm^{-1}
density of Promethium oxide source (ρ_{PM})	**half-life ($t_{0.5}$)**	**mean energy required to produce an electron-hole pair (w)**	**Specific activity at the beginning of life (H_0)**
6.6 g/cm^3	2.6 yr	3.67 *eV*	678 *Ci/g*
Silicon band gap (Eg)	**Density of Si (ρ_{si})**		
1.2 *eV*	2.33 g/cm^3		

Table 4. The basic battery parameters in three modes (without self-absorption, with self-absorption, and with both self-absorption and backscattering) for the conventional planar betavoltaic.

Parameter	**Considering the self-absorption**	**without considering the self-absorption and source backscattering**	**Considering the self-absorption and source backscattering**
Beta emission current at the surface of the source (μA)	13.064	19.093	18.721
Beta current at the p-n junction (μA)$\times e^{-ax}$	10.843	15.847	15.538
Rate of generation of electron-hole pairs in the semiconductor (#/cm^3.*sec*)$\times 10^{17} \times e^{-ax}$	1.797	2.627	2.576
Short circuit current density (A/cm^2)$\times 10^{-4}$	0.7565	1.106	1.084
Open-circuit voltage (V)	0.5699	0.5797	0.5792
Fill Factor	0.8208	0.8230	0.8223
Observable activity of thin sample (Ci)	5.460	7.980	7.824
Source power (W) $\times 10^{-3}$	2.360	3.449	3.381
Overall efficiency (%)	4.274	4.361	4.352

Table 4 illustrates the influence of self-absorption and backing material on critical parameters, including the beta emission current at the source surface, beta current at the p-n junction, the generation rate of electron-hole pairs within the

semiconductor, short circuit current density, open-circuit voltage, Fill Factor, observable activity of the thin sample, source power, and overall efficiency of the ^{63}Ni planar betavoltaic cell under investigation.

According to the second row of **Table 4**, self-absorption results in a reduction of approximately 6 μA in the beta emission current at the source surface. By neglecting the self-absorption effect in the backing material, it can be observed that the backscattering effect compensates for this decline, resulting in a net reduction of 5 μA. Because in real batteries, the effects of self-absorption and backscattering are inevitable, the third column of **Table 4** presents more accurate data for real cells. In each row, the effect of self-absorption and backscattering can be seen in reducing and increasing the corresponding parameter, respectively.

As demonstrated in **Table 4**, the phenomenon of self-absorption loss can result in a reduction of actual activity by as much as 46% when self-absorption and source dispersion are not taken into account. This can greatly affect the overall efficiency. Considering the effect of self-absorption loss, the efficiency of the battery is up to 1.99% less than when both self-absorption and source backing factors are ignored. With both self-absorption and source backscattering factors, the cell's efficiency is 0.21% less than when these effects are overlooked. Therefore, it can be concluded that the source backscattering partially compensated for the negative effect of self–absorption on efficiency.

Within the framework of betavoltaic technology, the source of ionizing particles can be categorized as either a surface source, where the particles are coated on a transducer, or a volume source, where they are embedded within a solid medium. **Table 6**-(I) shows that the minimum volume for producing $3.45\times10^{-3}(W)$ in the case of the planar betavoltaic cell that we are concerned with is $6.73\times10^{10}(\mu m^3)$. For the spherical battery, the minimum volume required to produce the same amount of power is $6.55\times10^{9}(\mu m^3)$. A significant amount of energy is not utilized in the planar cell approach. Beta particles are emitted in a continuous energy spectrum in all directions; however, the effective beta energy that is converted is minimal, often less than fifty percent of the total beta energy. Thus, a substantial amount of beta radiation is wasted. The geometric structure of a spherical cell is such that there is no loss in directions other than the transducer, and for this reason, a spherical cell has the ability to produce a specific power in a smaller volume than a planar cell. The results of **Table 6** confirm that the smallest nuclear batteries are volumetric cell types [26].

Table 5. The stopping range of the source beta particles in the transducer.

Stopping range	**TIO**	**Katz and Penfold**	**Prelas**	**(K–O)**
***L*(*μm*)**	204.77	224	229.84	235.15

Table 6. Size parameters and minimum volume values of the planar and spherical cells calculated by **Eqs. (34-41)**. (I) The stopping range of beta particles of 147-Pm in semiconductor materials, L, is calculated by using the relationship given by Katz and Penfold. (II) L is calculated by using the relationship given by Tabata, Ito, and Okabe. (III) L is calculated by using the relationship developed by Prelas et al. (IV) L is calculated based on the formula developed by Kanaya–Okayama (K–O).

(I)

Planar cell		**Spherical cell**	
ITEM	**VALUES**	**ITEM**	**VALUES**
$FCS(\mu m)$	12.09	$FCS(\mu m)$	1874.26
$L(\mu m)$	224	$L(\mu m)$	224
$S_{min}(\mu m)$	236.09	$S_{min}(\mu m)$	2322.26
$V_{source}(\mu m)^3$	3.45×10^{9}	$A_{min,source+transducer}(\mu m)^3$	1.69×10^{7}
$V_{min,source+transducer}(\mu m)^3$	6.73×10^{10}	$V_{min,source+transducer}(\mu m)^3$	6.55×10^{9}

(II)

Planar cell		Spherical cell	
ITEM	**VALUES**	**ITEM**	**VALUES**
$FCS(\mu m)$	12.09	$FCS(\mu m)$	1874.26
$L(\mu m)$	204.77	$L(\mu m)$	204.77
$S_{min}(\mu m)$	216.86	$S_{min}(\mu m)$	2283.8
$V_{source}(\mu m)^3$	3.45×10^{9}	$A_{min,source+transducer}(\mu m)^3$	1.64×10^{7}
$V_{min,source+transducer}(\mu m)^3$	6.18×10^{10}	$V_{min,source+transducer}(\mu m)^3$	6.23×10^{9}

(III)

Planar cell		Spherical cell	
ITEM	**VALUES**	**ITEM**	**VALUES**
$FCS(\mu m)$	12.09	$FCS(\mu m)$	1874.26
$L(\mu m)$	229.84	$L(\mu m)$	229.84
$S_{min}(\mu m)$	241.93	$S_{min}(\mu m)$	2333.94
$V_{source}(\mu m)^3$	3.45×10^{9}	$A_{min,source+transducer}(\mu m)^3$	1.71×10^{7}
$V_{min,source+transducer}(\mu m)^3$	6.90×10^{10}	$V_{min,source+transducer}(\mu m)^3$	6.65×10^{9}

(IV)

Planar cell		Spherical cell	
ITEM	**VALUES**	**ITEM**	**VALUES**
$FCS(\mu m)$	12.09	$FCS(\mu m)$	1874.26
$L(\mu m)$	235.15	$L(\mu m)$	235.15
$S_{min}(\mu m)$	247.24	$S_{min}(\mu m)$	2344.56
$V_{source}(\mu m)^3$	3.45×10^{9}	$A_{min,source+transducer}(\mu m)^3$	1.73×10^{7}
$V_{min,source+transducer}(\mu m)^3$	7.05×10^{10}	$V_{min,source+transducer}(\mu m)^3$	6.74×10^{9}

In **Figs. 7-11**, the relationship between nominal source activity, the total number of source atoms, the overall power output generated by the radioactive source, the maximum energy of beta particles, and semiconductor density with cell dimensions for the spherical cell has been shown. As it is expected, there is a direct relationship between the source curie content and the total number of fuel atoms with the cell size. By assuming the same quality of battery components, a larger-sized cell is capable of generating more power, and the use of sources that emit higher energy beta particles will increase the size of the battery. On the other hand, the use of higher-density semiconductors reduces the size of the transducer and the entire cell.

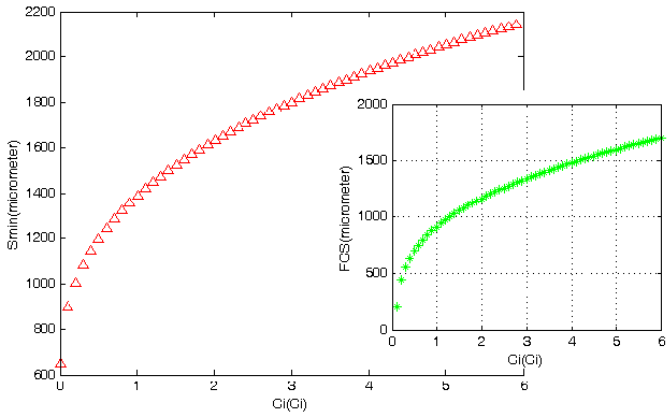

Fig. 7. Dependences of S_{min} (left) and FCS (right) on the nominal source curie content according to **Eqs. (33)** and **(38)** for the spherical cell.

Advances in Energy Science and Technology
Vol. 1, No. 2|1 September 2025
AEST

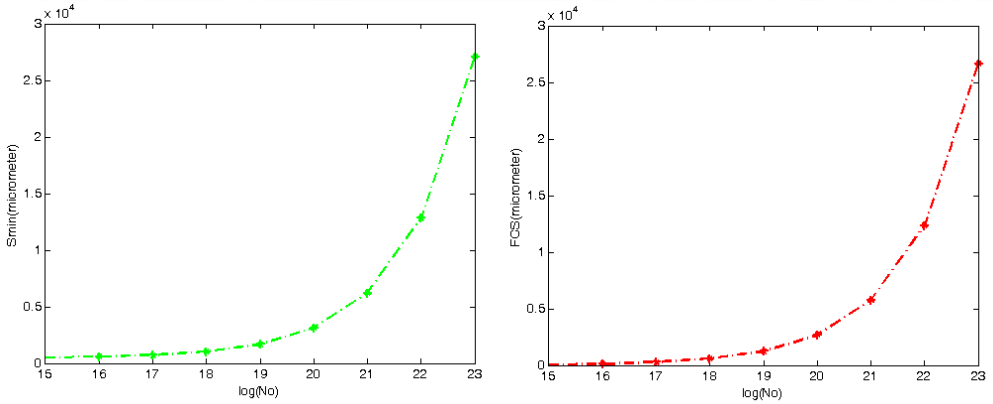

Fig. 8. Effect of the total number of source atoms in the cell's volume on S_{min} (left) and FCS (right) according to **Eqs. (33)** and **(38)** for the spherical cell. It should be noted that the relationship between S_{min} and N_0 is $S_{min-spherical\ cell}(\mathrm{I}) = 2[\left(\frac{3P\tau V}{4\pi E_{av}N_0}\right)^{\frac{1}{3}} + \frac{0.412}{\rho}E_{\beta,max}{}^{1.265-0.0954Ln(E_{\beta,max})}]$.

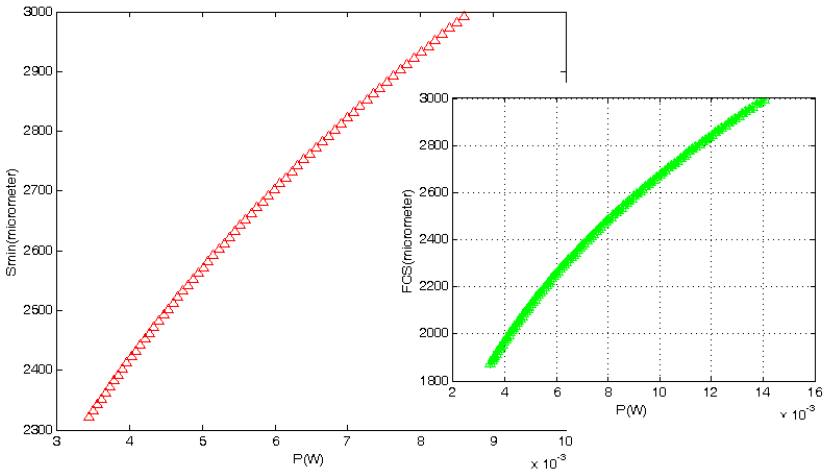

Fig. 9. S_{min} (left) and FCS (right) as a function of power according to **Eq. (33)** and **Eq. (38)** for the spherical cell.

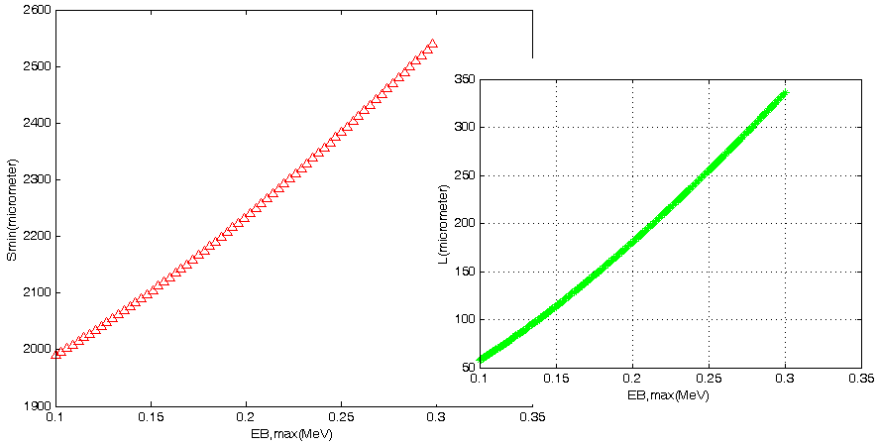

Fig. 10. S_{min} (left) and L (right) versus maximum energy of beta particles according to **Eq. (26)** and **Eq. (38)** for the spherical cell.

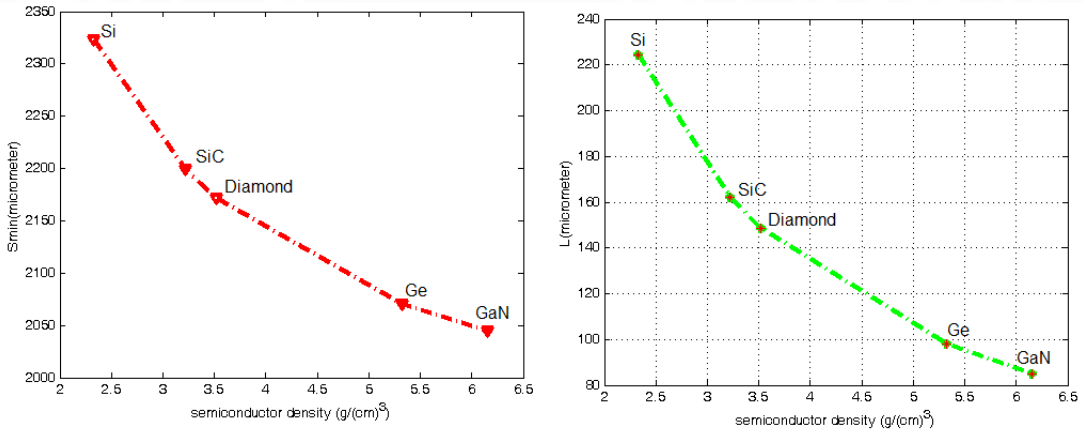

Fig. 11. S_{min} (left) and L (right) versus semiconductor density according to **Eq. (26)** and **Eq. (38)** for the spherical cell.

4. Conclusion

This study examined the effects of two source phenomena, self-absorption and source backscattering, on the efficiency of a 147-Pm planar betavoltaic cell. The findings indicate that self-absorption negatively impacts all fundamental cell parameters, resulting in a decrease in battery performance from 4.361% to 4.274% (a relative reduction of 1.99%). When both phenomena are considered in calculations, the efficiency becomes more accurate, reaching up to 4.352%. The research also demonstrated the relationship between the smallest possible dimensions of planar and spherical 147-Pm betavoltaic cells and key battery variables, including power, radioactive atom mean lifetime, beta particle average and maximum energy, radioisotope atomic density, source curie content, and transducer density. To generate 3.45×10^{-3} (W) power, the minimum required volume for planar and spherical cells was 6.73×10^{10} and 6.55×10^{9}, respectively. In planar batteries, over half of the beta particles are emitted in the wrong direction, necessitating a larger volume compared to spherical batteries to produce equivalent power output.

Author contributions

H.F. developed the theoretical formalism and wrote the paper, **F.A.D.** conceived the idea, designed the study**, M.A.** conceptualized the research, **H.A.** supervised the project, directed the research, and revised the manuscript.

Declaration of competing interest

The authors declare that they have no known competing financial interests or personal relationships that could have appeared to influence the work reported in this paper.

References

[1] L.C. Olsen, S.E. Seeman, B.I. Griffin, Betavoltaic nuclear electric power sources, Trans. Am. Nucl. Soc. 12 (1969) 481–482.

[2] P. Rappaport, The electron-voltaic effect in p-n junctions induced by beta-particle bombardment, Phys. Rev. 93 (1954) 246–247.

[3] W. Ko, J. Hynecek, Implant evaluation of a nuclear power source betacel battery, IEEE Trans. Biomed. Eng. 21 (1974) 238–241.

[4] F. Huffman, J. Norman, Nuclear-fueled cardiac pacemakers, Chest 65 (1974) 667–672.

[5] L. Wei, Parametric studies and optimization of the beta-voltaic cell—I. Short-circuit current, Solid-State Electron. 17 (1974) 1091–1098.

[6] L. Wei, Parametric studies and optimization of the beta-voltaic cell—II. Open-circuit voltage and power efficiencies, Solid-State Electron. 18 (1975) 71–77.

[7] H. Guo, A. Lal, Nanopower betavoltaic micro batteries, Proc. Solid-State Sens. Actuators Microsyst. 1 (2003) 36–39.

[8] W. Sun, N.P. Kherani, K.D. Hirschman, L.L. Gadeken, P.M. Fauchet, A three-dimensional porous silicon p-n diode for betavoltaics and photovoltaics, Adv. Mater. 17 (2005) 1230–1233.

[9] B. Liu, K.P. Chen, N.P. Kherani, S. Zukotynski, Power-scaling performance of a three-dimensional tritium betavoltaic diode, Appl. Phys. Lett. 95 (2009) 233112.

[10] C. Eiting, V. Krishnamoorthy, S. Rodgers, T. George, J.D. Robertson, J. Brockman, Demonstration of a radiation resistant, high-efficiency SiC betavoltaic, Appl. Phys. Lett. 88 (2006) 064101.

[11] R. Duggirala, S. Tin, A. Lal, 3D silicon betavoltaics microfabricated using a self-aligned process for 5 milliwatts/cc average, 5-year lifetime micro batteries, Proc. Int. Conf. Solid-State Sens. Actuators Microsyst. (2007) 279–282.

[12] Q. Da-Yong, Y. Wei-Zheng, G. Peng, Y. Xian-Wang, Z. Bo, Z. Lin, G. Hui, Z. Hong-Jian., Demonstration of a 4H SiC betavoltaic nuclear battery based on Schottky barrier diode, Chin. Phys. Lett. 25 (2008) 3798–3800.

[13] D.-Y. Qiao, X.-J. Chen, Y. Ren, W.-Z. Yuan, A micro nuclear battery based on SiC Schottky barrier diode, J. Microelectromech. Syst. 20 (2011) 685–690.

[14] Z. Cheng, H. San, Y.Li, X. Chen, The design optimization for GaN-based betavoltaic micro battery, Proc. IEEE Int. Conf. Nano/Micro Eng. Mol. Syst. (2010) 582–586.

[15] A. Jaffey, Solid angle subtended by a circular aperture at point and spread sources: formulas and some tables, Rev. Sci. Instrum. 25 (1954) 349.

[16] A. Masket, Solid angle contour integrals, series, and tables, Rev. Sci. Instrum. 28 (1957) 191.

[17] T. Tabata, R. Ito, S. Okabe, Nucl. Instrum. Methods 94 (1972) 509.

[18] N. Tsoulfanidis, Measurement and detection of radiation, Hemisphere Publ., 1995.

[19] V.A. Kuzminikh, S.A. Vorobiev, Nucl. Instrum. Methods 129 (1975) 561.

[20] H. Flicker, J.J. Loferski, T.S. Elleman, IEEE Trans. Electron Devices 11 (1964) 2.

[21] J.H. Jarrett, H.H. Van Tuyl, Promethium Isotopic Power Data Sheets, Battelle Memorial Institute, May 1970.

[22] S. Shionoya, W.M. Yen (Eds.), Phosphor Handbook, CRC Press, Boca Raton, FL, 1999.

[23] C. Thomas, S. Portnoff, M.G. Spencer, High efficiency 4H-SiC betavoltaic power sources using tritium radioisotopes, Appl. Phys. Lett. 108 (2016) 013505.

[24] X.B. Tang, Y.P. Liu, D. Ding, D. Chen, Optimization design of GaN betavoltaic microbattery, Sci. China Technol. Sci. 55 (2012) 659–664.

[25] K. Kanayat, S. Okayama, Penetration and energy-loss theory of electrons in solid targets, J. Phys. D: Appl. Phys. 5 (1972) 43.

[27] T.Wacharasindhu, Nullmeyer, B.R., Kwon, J.W., Robertson, J.D., Garnov, A.Y., Mechanisms leading to losses in conventional beta-voltaics and evolution utilizing composite semiconductor with infused radioisotope for efficiency improvement, J. Micro. Electro. Mech. Sys. 23 (2014) 56–65.